



Original Paper

Effect of existence state of asphaltenes on the asphaltenes-wax interaction in wax deposition



Yun Lei, Han Wang, Shuang-Shuang Li, Xue-Qian Liu, Hao-Ran Zhu^{**}, Yu-Ming Gao, Hao-Ping Peng, Peng-Fei Yu^{*}

Jiangsu Key Laboratory of Oil and Gas Storage □ Transportation Technology, Changzhou University, Jiangsu, 213164, China

ARTICLE INFO

Article history:

Received 16 May 2022

Received in revised form

23 August 2022

Accepted 23 August 2022

Available online 29 August 2022

Edited by Xiu-Qiu Peng

Keywords:

Asphaltenes

Precipitation/aggregation

Existence state of asphaltenes

Deposition

ABSTRACT

Asphaltenes are the most elusive substances in waxy crude oil, especially the complex structures, which leads to significant precipitation and aggregation characteristics of asphaltenes, and affects the asphaltenes-wax interaction. In this study, the concept of the existence state of asphaltenes was introduced to semi-quantitatively investigate the precipitation and aggregation characteristics of asphaltenes. On this basis, the influence of the existence state of asphaltenes on wax deposition was studied by coldfinger device and high-temperature gas chromatography, and the composition and properties of the deposits were analyzed. Four main findings were made: (1) As the asphaltene concentration increases, the existence state of asphaltenes gradually transitions from dispersed state to aggregated state, and the asphaltene concentration of 0.30 wt% in this study is the starting point of the transition. (2) The existence state of asphaltenes in crude oil does affect the process of wax deposition, as shown in the fact that the dispersed asphaltenes promote the occurrence of wax deposition, while the aggregated asphaltenes can inhibit wax deposition. (3) In the presence of the aggregated asphaltenes, that is, when the asphaltene concentration is higher than 0.30 wt%, the shedding phenomenon of deposit layer was observed, and with the increase of aggregated asphaltenes, the deposit layer fell off earlier. (4) With the increase of the dispersed asphaltenes, the wax appearance temperature (WAT) and wax content of the deposits all showed an increasing trend, while with the appearance of the aggregated asphaltenes, the above situation was reversed. The findings of this study can help for better understanding of the interaction between the asphaltenes and wax in wax deposition.

© 2022 The Authors. Publishing services by Elsevier B.V. on behalf of KeAi Communications Co. Ltd. This is an open access article under the CC BY-NC-ND license (<http://creativecommons.org/licenses/by-nc-nd/4.0/>).

1. Introduction

With the decreasing of oil and gas resources in onshore and offshore areas, the deepwater areas will be the focus of global oil and gas in the 21st century (Aiyejina et al., 2011). The development of the deepwater oil and gas is full of opportunities but also faces many challenges. Under the harsh conditions of high pressure, low temperature and strong heat exchange, the flow problems such as the waxes, asphaltenes and hydrate seriously threaten the safe operation of production systems (Valinejad and Nazar, 2013; Bai and Zhang, 2013; Cheng et al., 2022; Li et al., 2017). One of the

most important aspects is the deposition problem under the coexistence of the asphaltenes and waxes, which has attracted widespread attention in petroleum industry (Shetty et al., 2019; Olayiwola and Dejam, 2019; Mirshekar et al., 2020).

As an important component of crude oils, asphaltenes are defined that are insoluble in normal paraffins with low molecular weight such as pentane and heptane, but can dissolve in aromatic substances such as benzene and toluene. Under no external influences, such as the temperature, pressure and composition, it is as a single phase in crude oils in the form of colloidal particles (Rogel, 2016; Choi et al., 2016; Redelius, 2004; Zhao and Shaw, 2007). Once the above effects exist, the asphaltenes in colloidal form can precipitate and aggregate from crude oils or model oils (Taheri et al., 2019; Shahebrahimi and Fazlali, 2018; Li et al., 2018; Guzmán et al., 2017; Chen et al., 2018; Davudov and Moghanloo, 2019; Fávero et al., 2017; Nategh et al., 2018). Due to the unique properties

* Corresponding author.

** Corresponding author.

E-mail addresses: zhuhaoran@cczu.edu.cn (H.-R. Zhu), yupengfei@cczu.edu.cn (P.-F. Yu).

of asphaltenes, the asphaltenes-wax interaction in waxy oils has been studied for nearly two decades. Kriz et al. introduced that the WAT and yield stress of system can be significantly increased when the asphaltene concentration was 0.01 wt%; As the asphaltene concentration increases to 0.02 wt%, WAT and yield stress decrease significantly (Kriz and Andersen, 2005). Venkatesan et al. also found that the presence of asphaltenes could affect the strength of gelling structure of the waxy oil by reducing the gelation temperature and yield stress, and they identified the effect of the aliphatic hydrocarbon with the weakest polar in asphaltenes on the reduction of gelation temperature (Venkatesan et al., 2003). Li et al. further reported that when there is no asphaltenes in the system, the wax crystals precipitated are needle-like, and a continuous network of wax crystals can be easy to form. However, when asphaltenes were added, the entire waxy oil exhibits spherical flocculation, which is beneficial to the Brownian diffusion of asphaltenes and the molecular diffusion of wax (Li et al., 2016; Yang et al., 2016). Oliveira et al. showed that asphaltenes can act like a pour point depressant, but has almost no effect on WAT (Oliveira and Lucas, 2007).

Researchers have also observed significant influences by the asphaltenes on the process of wax deposition. Tinsley et al. found that the wax deposition rate in model oils was reduced when the added asphaltene concentration was up to 0.20 wt%. In addition, they further discovered that the asphaltene concentration in deposits is also 10 times higher than that in original model oil (Tinsley, 2008; Tinsley and Prud'homme, 2010; Tinsley et al., 2007). Yao also proposed that the asphaltene concentration in deposit can reach almost 3 times than that of original oil by traditional cold finger apparatus, which is consistent with the observations by Tinsley et al. (Yao, 2014). Li et al. observed that under the low asphaltene concentrations, two-layer deposits with varying structural strengths were formed. The inner layer is solid-like with higher WAT, wax content and asphaltene content. On the contrary, the outer layer is loosely gelatinized and have lower WAT, wax content and asphaltene content (Li et al., 2016; Yang et al., 2016). Lei et al. found that there is a “critical concentration” between the wax deposition rate and asphaltene concentration. When the asphaltene concentration is lower than the critical value, the wax deposition rate increases with the increase of asphaltene concentration; once the asphaltene concentration is higher than the critical value, the wax deposition rate decreases with the increase of asphaltene concentration. They believed that the existence state of asphaltenes is the main factor determining the wax deposition rate, but it is not clear how the existence state of asphaltenes works (Lei et al., 2016). Li et al. found that compared with the absence of asphaltenes, the wax deposition rate decreased in the presence of asphaltenes, but the content of wax and asphaltene increased in deposits, and the asphaltene content was several times than that of the asphaltene content in original oil sample. In addition, they observed deposits slough off at higher asphaltene concentrations (Li et al., 2020).

Admittedly, most of the current research mainly focus on the effect of asphaltene type and concentration on wax deposition, while few studies involved to reveal the influence of existence state of asphaltenes. To this end, this study carried out an in-depth study on the effect of existence state of asphaltenes on wax deposition. Firstly, the asphaltenes structure was characterized by Fourier transform infrared spectroscopy (FTIR). In addition, the differences in the existence state of asphaltenes were achieved by varying the asphaltene concentration added to waxy crude oil, and the microscopic observation and software analysis were used to obtain the size distribution of asphaltenes and semi-quantitatively characterize the existence state of asphaltenes. Moreover, a series of coldfinger deposition experiments were carried out, and deposit characteristics were also analyzed by DSC and High-temperature

gas chromatography (HTGC).

2. Experimental section

2.1. Experimental materials

One typical waxy crude oil (wax content of 15.36 wt%) that has very little asphaltenes was used. The physical properties are shown in Table 1, in which the SARA analysis of waxy crude oils is based on the criterion of ASTM6560-17, the mass error of nC7-asphaltene is within 5%, and the mass error of other components is within 10%. The wax precipitation characteristics is shown in Fig. 1. In addition, other chemicals, such as the n-heptane and toluene, etc., were purchased from the Sinopharm Chemical Reagent Co., Ltd. (China), and all chemicals used in this study are of analytical grade.

2.2. Experimental apparatus

2.2.1. Fourier transform infrared spectroscopy

Nicolet iS50 Fourier Transform Infrared Spectrometer from Thermo Fisher was adopted to characterize the asphaltenes structure. During the process, an appropriate amount of asphaltenes and dry KBr were mortared evenly in an agate. After the mixture being put into a mold, the pressure was controlled under 15 MPa for 2 min, and the pressed tablet was taken out and placed in a high-pressure mercury lamp to dry for 30 min before testing. The wave number range of experimental scan is between 4000 and 400 cm^{-1} , and the scan number is 120 times.

2.2.2. DSC measurements

The wax precipitation characteristics and wax content of crude oils and deposits were obtained using DSC equipment (TA20) and followed the method presented by Chen et al. (2004). During the process, the samples were firstly heated to 80 °C, and maintained for 5 min, and then cooled to –20 °C at a cooling rate of 5 °C/min. The heat generated due to wax precipitation can be tested. Note that all samples are tested for triplicate repeatability for accuracy. The average of three results is taken as the final result. The accuracy of WAT measurements is within 1 °C, and the repeatability of wax content is within 4%.

2.2.3. Coldfinger apparatus

A coldfinger apparatus is used to analyze the wax deposition of waxy crude oil considering the effect of existence state of asphaltenes, as shown in Fig. 2. The coldfinger apparatus consists of the following: a coldfinger to provide wax deposition surface, a hot water bath to provide the temperature of crude oil, a cold-water bath to maintain the temperature of coldfinger, and a stainless-steel inner cavity for the storage of crude oil. The water bathes used is HAAKE F3, and the temperature-controlled precision is within 0.1 °C. In deposition experiments, the temperatures of crude oil and coldfinger surface were adjusted to form temperature gradient between them, which in turn controlled the entire wax deposition process.

Table 1
Physical properties of waxy crude oils used in this study.

Physical properties	Waxy crude oil
Density @ 20 °C, kg/m^3	818
WAT, °C	40
Saturate, wt.%	76.6
Aromatic, wt.%	20.1
Resin, wt.%	3.2
nC7-asphaltene, wt.%	0.1

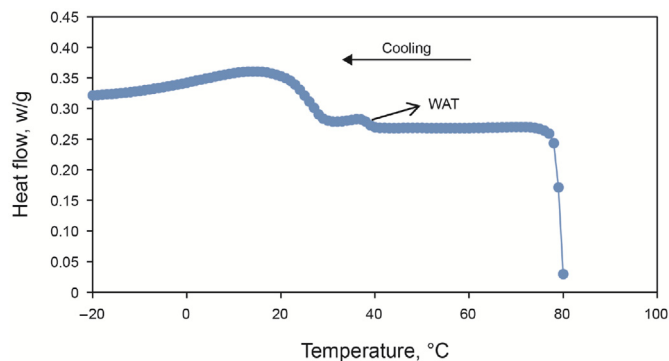


Fig. 1. Thermal spectra curve of the crude oil during cooling.

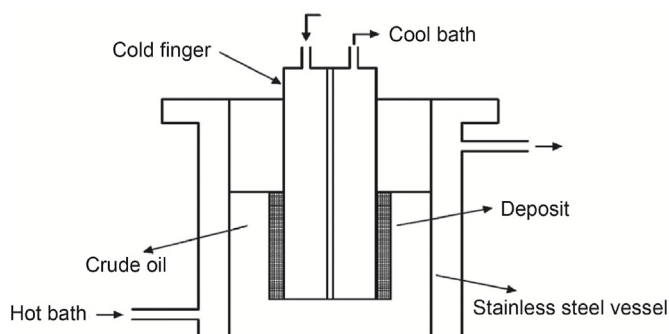


Fig. 2. Sketch of the coldfinger apparatus.

2.2.4. High-temperature gas chromatography

High-temperature gas chromatography is used to analyze the n-alkane composition of deposits. The device comes from the AC high-temperature SIMDIS equipped with Agilent 6890N GC. In addition, the analysis method was performed using the AC HT-750a method.

2.3. Experimental procedure and method

2.3.1. Asphaltene extraction

In this study, the asphaltene extraction adopts the n-heptane precipitation method to obtain the required asphaltenes from Venezuelan vacuum residue. The specific steps of asphaltene extraction are as follows:

- (1) To extract as much asphaltenes from crude oil as possible, sufficient amount of n-heptane is mixed into the Venezuelan vacuum residue in a ratio of 40 mL:1 g.
- (2) After 30 min, the mixture was filtered using a glass filter with a pore size of 10–15 μm , and then the obtained filter cake was dissolved in toluene.
- (3) After a period of time, the toluene solution containing asphaltenes was evaporated in a vacuum oven to remove the toluene. After that, the obtained asphaltene cake is washed using an appropriate amount of hot n-heptane to remove the non-asphaltene components for three times.
- (4) The retained asphaltenes were dried under nitrogen flow and stored in a closed dark environment.

2.3.2. Optical microscopy and existence state of asphaltenes

Optical microscopy was used to observe and analyze the

existence state of asphaltenes. The experiment procedure and method can be seen in our previous work (Lei et al., 2016). It should be noted that the microscopic images of asphaltenes were taken at 55 $^{\circ}\text{C}$, which is 15 $^{\circ}\text{C}$ higher than the WAT of oil samples to eliminate the interference of wax crystals. In addition, 15 micrographs (2048×1536 pixels) were obtained and saved to count the size distribution of asphaltenes for each sample, and the second repeated experiment was also done.

2.3.3. Coldfinger deposition experiment

In coldfinger deposition experiment, the crude oil was firstly heated to 55 $^{\circ}\text{C}$ to ensure that no wax is precipitated from the oil sample. In addition, 800 g of crude oil was poured into the stainless-steel vessel, which is sufficient to avoid significant changes in the wax precipitation characteristics during wax deposition. The temperatures of crude oil and coldfinger were respectively controlled at 55 and 30 $^{\circ}\text{C}$. In this case, it can generate a temperature driving force of 25 $^{\circ}\text{C}$ between the crude oil and coldfinger. Note that the deposition time lasted for 36 h, and the deposition of each oil sample was analyzed at 5 h, 10 h, 15 h, 20 h, 25 h and 36 h, respectively. Three repeated experiments were carried out under same conditions, and the average value of the three results was used as the final result.

3. Results and discussion

3.1. Characterization of asphaltene structure

The structure of asphaltenes determines their properties, which also affects their existence state in crude oils. Fig. 3 shows the FTIR spectra of asphaltene structure. It can be found that 10 distinct absorption peaks can be seen. For example, the first peak appears at about 3382.3 cm^{-1} in the wavenumber of fundamental frequency range, which indicates that the asphaltenes contain amine bonds (N–H); the aliphatic ether bonds (R–O–R') absorption peak appears at 1133.2 cm^{-1} ; the absorption peak of sulfoxide group (S=O) appears at about 1032.6 cm^{-1} . In addition, the rest of the absorption peaks (2922.5 cm^{-1} , 2852.1 cm^{-1} , 1457.8 cm^{-1} , 1375.8 cm^{-1}) in the fundamental frequency region represent the stretching vibration of methyl or methylene, while the absorption peaks (864.7 cm^{-1} , 803.3 cm^{-1} , 738.8 cm^{-1}) represent the stretching vibration of the benzene ring or aromatic branched chains. The elemental analysis of asphaltenes is shown in Table 2.

3.2. Existence state of asphaltenes in waxy crude oil

In this study, we added different concentrations of asphaltenes to crude oil, and the quality of crude oil is fixed, so as to form different existence states of asphaltenes. In order to quantitatively

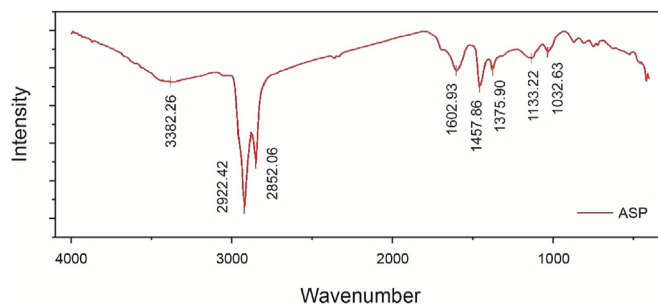


Fig. 3. Fourier transform infrared spectroscopy of n-heptane asphaltenes used in this study.

Table 2
Elemental analysis of asphaltenes.

Element	Mass fraction, wt.%
C	85.53
H	6.328
O	1.34
N	2.14
S	1.47

characterize the existence state of asphaltenes, two aspects of work were carried out: First, the microphotographs of asphaltenes were taken; second, the size distribution of asphaltenes in crude oil was quantified. Fig. 4 shows the micrograph of asphaltenes at different asphaltene concentrations, and the black dots represent the asphaltenes captured in the field of view.

It can be seen that as the asphaltene concentration increases, the number of asphaltenes that can be captured in the field of view also increases. Interestingly, when the asphaltene concentration exceeds 0.30 wt%, the morphology of visible asphaltenes changes significantly compared to the case below this concentration, and the most obvious feature is that the size of visible asphaltenes increases sharply, and asphaltene particles appear as lumps or clusters. However, when the asphaltene concentration is lower than this concentration, the asphaltene morphology is almost unchanged, only reflected in the increase in number. To this end, combined with the precipitation and aggregation characteristics of asphaltenes, we put forward the concept of existence state of asphaltenes to explain the reasons for the morphological changes of asphaltenes in crude oil.

Fig. 5 shows a schematic diagram of the existence state of asphaltenes as a function of asphaltene concentration. Here, on the basis of previous research, we introduce the concepts of dispersed asphaltenes and aggregated asphaltenes. When the asphaltene concentration added to the crude oil is small, according to the similar compatibility theory, the aromatic components in crude oil can play a good dispersing effect on asphaltenes, and the interaction between asphaltene monomers is not significant. In this case, asphaltenes appear to be evenly dispersed in crude oil, and the

asphaltenes in this existence state are called dispersed asphaltenes, which is the first stage of Fig. 5. With the increase of asphaltene concentration, the aromatic components in crude oil continually disperse asphaltenes, and the dispersed asphaltenes gradually increase, as shown in the second stage of Fig. 5. However, once the asphaltene concentration increases beyond the dispersing ability of aromatic components, coupled with the increase in number of dispersed asphaltenes per unit volume of crude oil, the interaction probability between dispersed asphaltenes increases, such as the collision, interaction between surface functional groups and electrostatic interaction, the local interactions between dispersed asphaltenes gradually occurs, which is manifested as “asphaltene precipitation”. As more asphaltene precipitation intensifies, the asphaltene aggregation occurs, which is directly reflected in the morphology change of asphaltenes, especially the sharp change of apparent size. This phenomenon can be represented in the third stage of Fig. 5. At this point, the dispersed asphaltenes are transformed into aggregated asphaltenes.

In order to further quantify the existence state of asphaltenes, the size distribution of asphaltenes is shown in Fig. 6. Interestingly, we found that 3 μm can be used as the dividing line between dispersed and aggregated asphaltenes. When the asphaltene concentration is lower than 0.30 wt%, the asphaltenes are all dispersed and their size are less than 3 μm . However, with the further increase of asphaltene concentration, the aggregated asphaltenes gradually appeared and increased, reflecting that the size distribution of asphaltenes tends to increase in large size (>3 μm), which is also consistent with the microscopic results.

3.3. Effect of existence state of asphaltenes on deposition rate and the aging of the deposits

3.3.1. Wax deposit mass

In Section 3.2, we quantified the existence state of asphaltenes in crude oil, which is also the basis for the study of wax deposition in this study. Fig. 7 shows the relationship between the wax deposit mass and asphaltene concentration after 36 h of coldfinger deposition. It can be seen that at this time, the deposit mass shows a

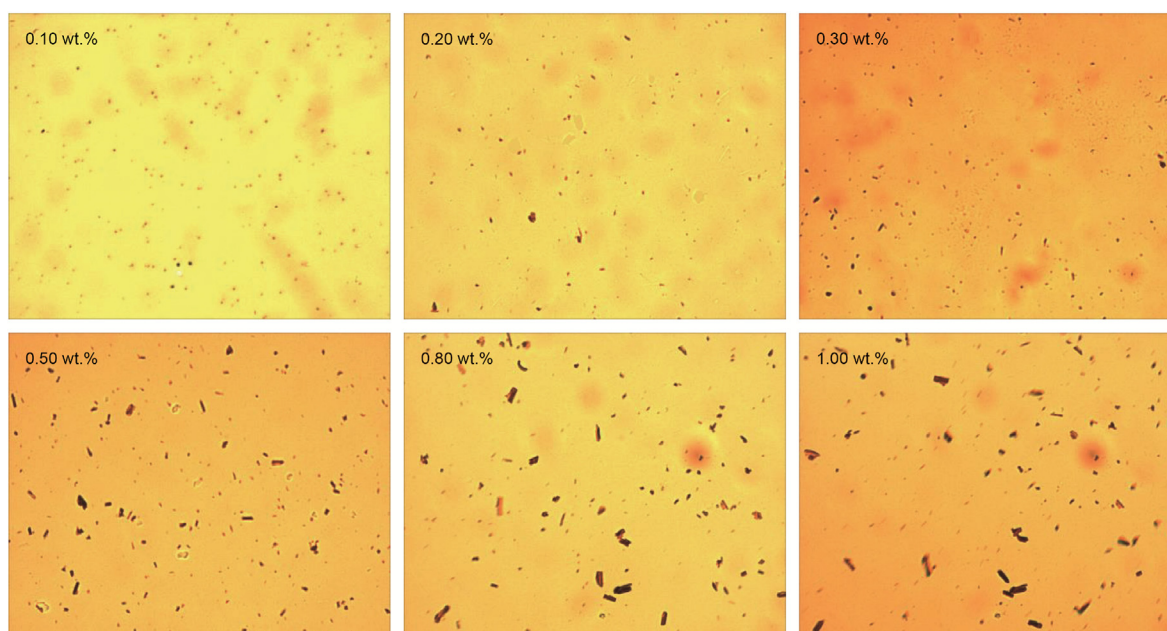


Fig. 4. Optical microscopic images of asphaltenes in crude oils (the black spots).

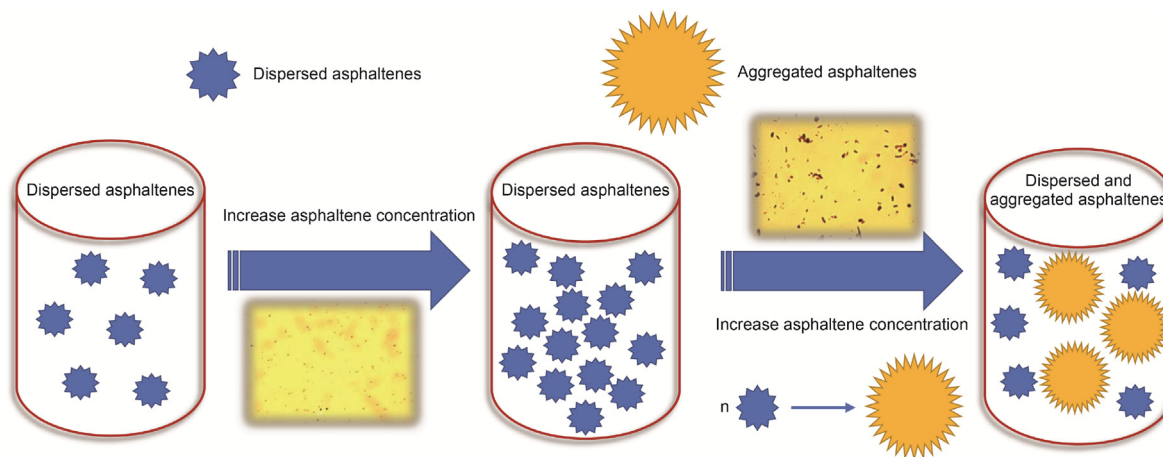


Fig. 5. Schematic diagram of the existence state of asphaltenes with the asphaltene concentration.

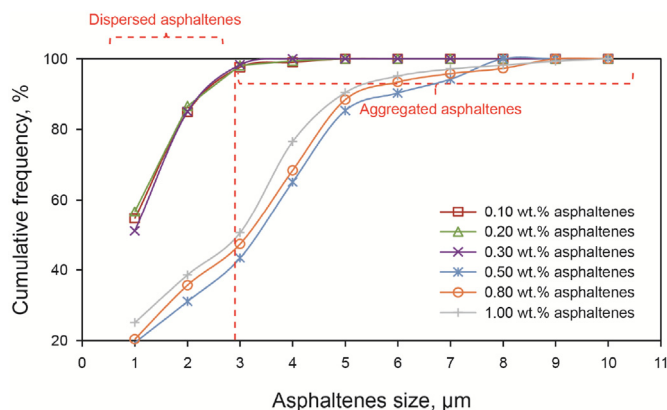


Fig. 6. Asphaltene particle size distribution for crude oils with varying asphaltene concentrations.

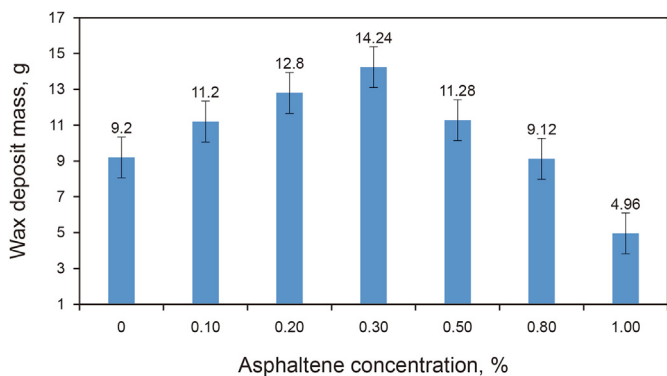


Fig. 7. Wax deposit mass with for crude oils with different asphaltene concentrations after 36 h.

variation law of first increase and then decrease. When the asphaltene concentration is 0.30 wt%, the deposit mass reaches the maximum at this time, and coincidentally, this concentration is also the starting point of the transformation of existence state of asphaltene from the dispersed state to aggregated state. Moreover, it is interesting to note that with the increase of dispersed asphaltene, the deposit mass gradually increased, but when a large amount of aggregated asphaltene is present (at asphaltene

concentration of 1.0 wt%), the deposit mass (4.96 g) is much smaller than the case where no asphaltene is present (9.2 g). In other words, it means that the existence state of asphaltene affects the wax deposition process, i.e., dispersed asphaltene contributes to wax deposition, while aggregated asphaltene inhibits wax deposition from occurring.

In order to further grasp the influence of the existence state of asphaltene, we analyzed the deposit mass in multiple deposition times under each asphaltene concentration, as shown in Fig. 8. It can be found that when the asphaltene exists in the dispersed state, the deposit mass increases with the increase of dispersed asphaltene and the prolongation of deposition time, as shown in Fig. 8a. However, once the aggregated asphaltene appeared, the deposit mass decreases with the increase of aggregated asphaltene in each deposition time period, as shown in Fig. 8b. In addition, a very strange phenomenon can also be found. Corresponding to the three cases of asphaltene concentrations of 0.5 wt%, 0.8 wt% and 1.0 wt%, we found that the deposit mass did not simply increase gradually with deposition time, but existed transition point of deposit mass reduction (indicated by the dashed red box in Fig. 8b). Moreover, with the increase of aggregated asphaltene, the transition point of deposit mass reduction corresponds to the earlier deposition time. It is also confirmed that the dispersed asphaltene and aggregated asphaltene have different effects on wax deposition.

As is known to all, the strength of wax deposition process mainly depends on the influence of the concentration gradient of wax molecules. Our previous study also found that the asphaltene in different existence states did affect the crystallization characteristics of waxes. Therefore, in order to explain the influence of existence state of asphaltene on wax deposition, we firstly analyzed the concentration gradient of wax molecules in crude oils used in coldfinger deposition experiment. Fig. 9 illustrates a schematic diagram of the temperature field from the cold finger wall to 2 mm outside and the concentration gradient of wax molecules. First, in the temperature field, it can be found that in the longitudinal direction, because the bottom and upper part of the stainless steel container of coldfinger device has no insulation by hot water bath, resulting in part of the cold and hot crude oil convection up and down; Second, in the radial direction, there is an obvious temperature gradient only in a very small area outside the coldfinger (2 mm in this study).

In addition, for the convenience of expression, we denoted the concentration of all wax molecules in bulk oils as C_w (approximately equivalent to the wax content of crude oil 15.36 wt%), the concentration of wax molecules at 2 mm outside the coldfinger as

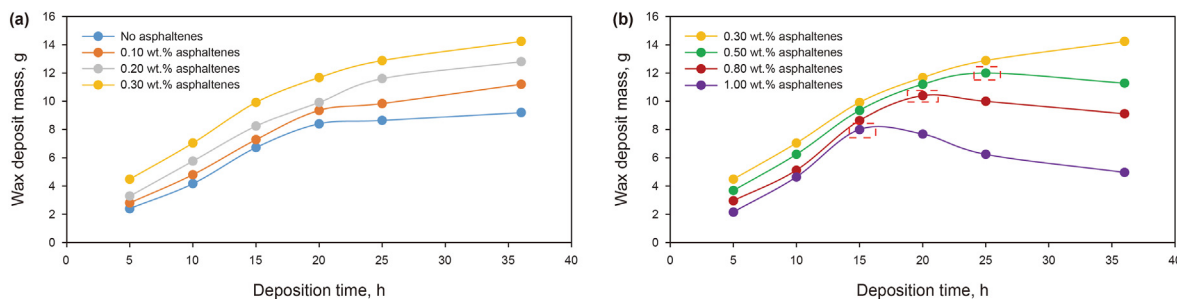


Fig. 8. Wax deposit mass with deposition time for crude oils with different asphaltene concentrations.

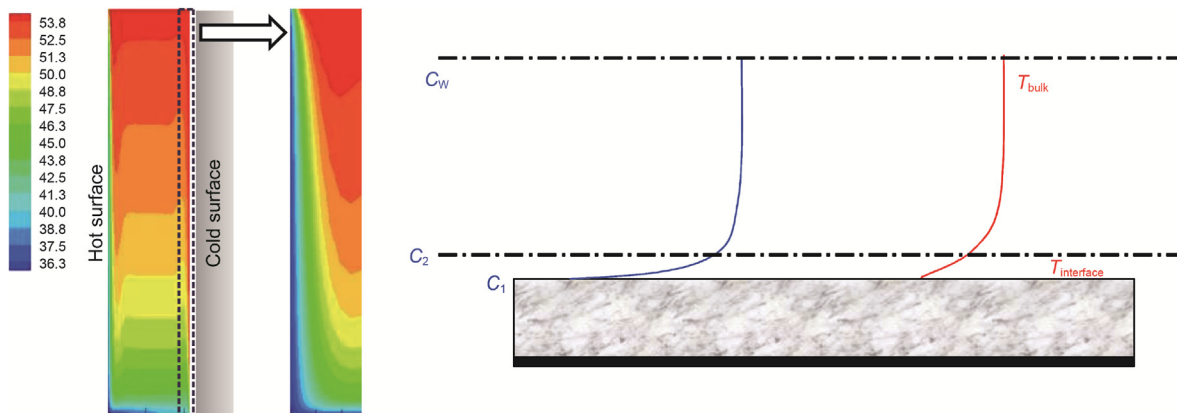


Fig. 9. Description of temperature field and concentration gradient of wax molecule near the coldfinger wall (2 mm).

C_2 , the concentration of wax molecules on the wall of coldfinger as C_1 , and the oil temperature of the bulk oils as T_{bulk} (55 °C), and the wall temperature of coldfinger as $T_{interface}$ (30 °C). Here, we assumed that the concentration of wax molecules on the surface of coldfinger is 0 at initial time of deposition and does not change as the deposition continues, that is, $C_1 = 0$. In addition, the concentration of wax molecules at C_2 is equal to the C_w minus the accumulated amount of wax precipitation at 40–30 °C. Therefore, according to the characteristics of wax precipitation (shown in Fig. 10), we can obtain the corresponding value at the case of each asphaltene concentration and concentration gradient of wax molecules, as shown in Table 3.

It can be seen from Table 3 that the concentration gradient of wax molecules in C_2 – C_1 region is much larger than that in C_w ~ C_2 region. In other words, during the process of wax deposition, the

Table 3

Concentration gradient of wax molecules in the C_w ~ C_2 and C_2 – C_1 regions.

	0.10%	0.20%	0.30%	0.50%	0.80%	1.00%
C_w	15.36%	15.36%	15.36%	15.36%	15.36%	15.36%
C_2	14.87%	15.07%	15.23%	14.72%	14.53%	14.36%
C_1	0	0	0	0	0	0
$(C_w - C_2) * 10^4 / 4.15$	11.81	6.99	3.13	15.42	20.00	24.10
$(C_2 - C_1) * 10^4 / 0.2$	7435	7535	7615	7360	7265	7180

concentration gradient of wax molecules is mainly controlled by C_2 – C_1 region, and it is obvious that the variation trend of the concentration gradient of wax molecules in this region is consistent with that of the deposit mass, that is, increase first and then decrease. Moreover, the cumulative concentration of wax precipitation in crude oils in Fig. 10 also shows the influence of existence state of asphaltenes on the wax precipitation characteristics, that is, the dispersed asphaltenes can inhibit the precipitation of wax molecule, while the aggregated asphaltenes can promote the precipitation of wax molecules, then resulting in the change in the concentration gradient of wax molecules between the bulk oils and deposition interface. The primary reason is that the aggregated asphaltenes can directly act as the crystallization core of wax molecules, which makes the wax precipitation process advance. However, the mechanism of the dispersed asphaltenes inhibiting wax precipitation is still unclear in this study, and further research is needed.

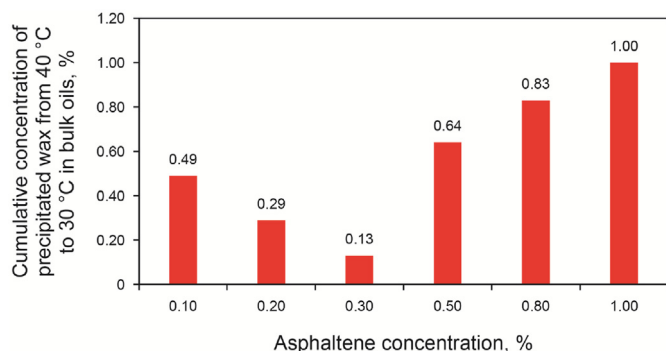


Fig. 10. Cumulative concentration of precipitated wax from 40 °C to 35 °C in bulk oils with varying asphaltene concentrations.

3.3.2. Wax precipitation characteristics of the deposits

The WAT and wax content of the deposits obtained from the coldfinger deposition experiments were characterized using DSC. Fig. 11 presents the results of the WAT and wax contents of the

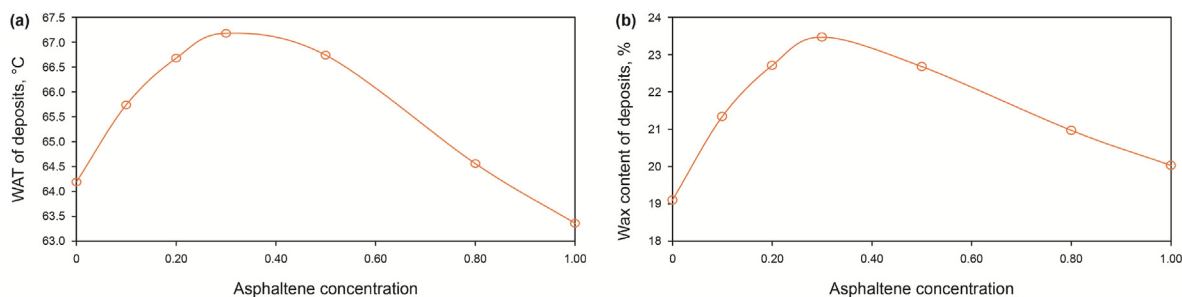


Fig. 11. Relationship between WAT and wax content of deposits when the deposition time is fixed at 36 h.

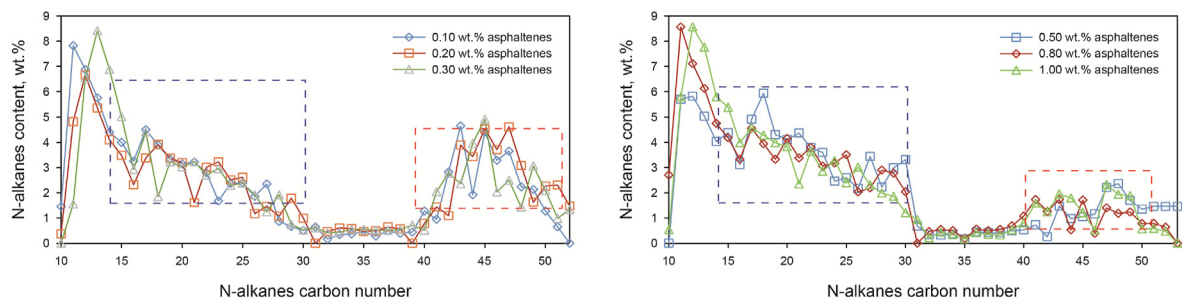


Fig. 12. N-alkanes content of deposits when the deposition time is fixed at 36 h.

deposits when the deposition time is fixed at 36 h. As can be seen from Fig. 11, when no aggregated asphaltene exists but only dispersed asphaltene, the WAT and wax content of the deposits continuously increase with the increase of the dispersed asphaltene. This trend can be explained by a mechanism of aging, in which internal diffusion of wax into the deposit causes the deposit to become increasingly wax-rich. However, when the aggregated asphaltene appeared, with the decrease of dispersed asphaltene and the increase of aggregated asphaltene, the WAT and wax content in deposits showed a downward trend. The main reason is the influence of the dispersed asphaltene and aggregated asphaltene on the concentration gradient of wax molecules in deposition experiments, which leads to the change of number and carbon number distribution of wax molecules diffused into the deposits.

3.3.3. N-alkane composition of deposits

In this study, the n-alkane carbon number distributions of the deposits were characterized using HTGC. Fig. 12 shows the n-alkane carbon number distributions of the deposits, and all deposits were obtained after 36 h deposition experiment. As can be seen from Fig. 12, the carbon number distribution in deposits mainly presents two regions: low-carbon number region (C10–C30, shown in blue dotted box) and high-carbon number region (C40–C50, shown in red dotted box). In addition, slight differences could be observed. For instance, when no aggregated asphaltene exists but only dispersed asphaltene, the content of high carbon number is significantly higher than that of the existence of aggregated asphaltene. However, when the aggregated asphaltene is present, the content of low-carbon waxes in deposits increases relatively. This is also consistent with the wax precipitation characteristics of deposits.

4. Conclusions

Currently, the influence of asphaltene on the wax deposition

has long been studied, yet whether the existence state of asphaltene would influence the process of wax deposition is an unresolved issue. With regard to this, by adding asphaltene into a waxy crude oil and forming dispersed asphaltene and aggregated asphaltene in waxy crude oils, this study shows that the existence state of asphaltene dose affect the process of wax deposition.

It was observed that when asphaltene is present in dispersed state, the dispersed asphaltene can inhibit the precipitation process of wax molecules, and increase the concentration gradient of wax molecules between the bulk crude oils and deposition interface. In the coldfinger deposition experiments, the deposit mass increases with the increase of the dispersed asphaltene. However, once the dispersed asphaltene is transformed into the aggregated asphaltene, the precipitation of wax molecules in bulk crude oils is promoted, and a large number of wax molecules lose the opportunity to diffuse to the deposition surface, resulting in the inhibition of wax deposition process. Furthermore, a shedding phenomenon of deposits was found, which is closely related to the presence of the aggregated asphaltene. It was found that the more the aggregated asphaltene, the earlier the deposit shedding. Moreover, we also demonstrate that the component of n-alkane in deposits is associated with the existence state of asphaltene. This work provides a fundamental understanding about the role of asphaltene in the process of wax deposition, and reveals the influence of the existence state of asphaltene on wax deposition, which is rarely considered in current studies.

Availability of data and material

The raw/processed data required to reproduce these findings cannot be shared at this time as the data also forms part of an ongoing study.

Declaration of competing interest

The authors declare that they have no known competing

financial interests or personal relationships that could have appeared to influence the work reported in this paper.

Acknowledgements

This work was supported by the National Natural Science Foundation of China (Grant No. 52174057), the Science and Technology Project of Changzhou City (Grant No. CJ20210136), the General Project of Natural Science Research in Jiangsu Universities (Grant No. 20KJB440004), and the Science and technology program of Changzhou University (Grant No. ZMF22020068).

References

- Aiyejina, A., Chakrabarti, D.P., Pilgrim, A., Sastry, M.K.S., 2011. Wax formation in oil pipelines: a critical review. *Int. J. Multiphas. Flow* 37 (7), 671–694. <https://doi.org/10.1016/j.ijmultiphaseflow.2011.02.007>.
- Bai, C.Y., Zhang, J.J., 2013. Effect of carbon number distribution of wax on the yield stress of waxy oil gels. *Ind. Eng. Chem. Res.* 52 (7), 2732–2739. <https://doi.org/10.1021/ie303371c>.
- Cheng, Q.L., Gan, Y.F., Wang, Z.H., Sun, W., Wang, S., Liu, C., Li, Q.B., Liu, Y., 2022. Molecular dynamics study on the radial deposition and adhesion process for the waxy crude oil tube transport system and effect-principle of features in construction. *Energy Fuels* 36, 310–319. <https://doi.org/10.1021/acs.energyfuels.1c03439>.
- Choi, S., Pyeon, W., Kim, J.D., Nho, S.S., 2016. Simple functionalization of asphaltene and its application for efficient asphaltene removal. *Energy Fuels* 30, 6991–7000. <https://doi.org/10.1021/acs.energyfuels.6b01184>.
- Chen, L., Meyer, J., Campbell, T., Canas, J., 2018. Applicability of simple asphaltene thermodynamics for asphaltene gradients in oilfield reservoirs: the Flory-Huggins-Zuo Equation of State with the Yen-Mullins model. *Fuel* 221, 216–232. <https://doi.org/10.1016/j.fuel.2018.02.065>.
- Chen, J., Zhang, J.J., Li, H.Y., 2004. Determining the wax content of crude oils by using differential scanning calorimetry. *Thermochim. Acta* 410 (1–2), 23–26. [https://doi.org/10.1016/S0040-6031\(03\)00367-8](https://doi.org/10.1016/S0040-6031(03)00367-8).
- Davudov, D., Moghanloo, R.G., 2019. A new model for permeability impairment due to asphaltene deposition. *Fuel* 235, 239–248. <https://doi.org/10.1016/j.fuel.2018.07.079>.
- Fávero, C.V.B., Maqbool, T., Hoepfner, M.P., Fogler, H.S., 2017. Revisiting the flocculation kinetics of destabilized asphaltenes. *Adv. Colloid Interface Sci.* 244, 267–280. <https://doi.org/10.1016/j.cis.2016.06.013>.
- Guzmán, R., Ancheytá, J., Trejo, F., Rodríguez, S., 2017. Methods for determining asphaltene stability in crude oils. *Fuel* 188, 530–543. <https://doi.org/10.1016/j.fuel.2016.10.012>.
- Kriz, P., Andersen, S.I., 2005. Effect of asphaltenes on crude oil wax crystallization. *Energy Fuels* 19, 948–953. <https://doi.org/10.1021/ef049819e>.
- Li, X.X., Guo, Y.M., Lan, W.J., Guo, X.Q., 2018. Effect of nanoparticles on asphaltene aggregation in a micro-sized pore. *Ind. Eng. Chem. Res.* 57 (27), 9009–9017. <https://doi.org/10.1021/acs.iecr.8b00729>.
- Li, C.X., Cai, J.Y., Yang, F., Zhang, Y., Bai, F., Ma, Y.Y., Yao, B., 2016. Effect of asphaltenes on the stratification phenomenon of wax-oil gel deposition formed in a new cylindrical coquette device. *J. Petrol. Sci. Eng.* 140, 73–84. <https://doi.org/10.1016/j.petrol.2016.01.004>.
- Li, M., Sun, M.R., Lu, Y.D., Zhang, J.J., 2017. Experimental study on the strength of original samples of wax deposits from pipelines in the field. *Energy Fuels* 31 (11), 11977–11986. <https://doi.org/10.1021/acs.energyfuels.7b02396>.
- Lei, Y., Han, S.P., Zhang, J.J., 2016. Effect of the dispersion degree of asphaltene on wax deposition in crude oil under static conditions. *Fuel Process. Technol.* 146, 20–28. <https://doi.org/10.1016/j.fuproc.2016.02.005>.
- Li, H.Y., Zhang, J.J., Xu, Q.G., Hou, C.Y., Sun, Y.D., Zhuang, Y., Han, S.P., Wu, C.C., 2020. Influence of asphaltene on wax deposition: deposition inhibition and sloughing. *Fuel* 266, 117047. <https://doi.org/10.1016/j.fuel.2020.117047>.
- Mirshakar, F., Pakzad, L., Fatehi, P., 2020. An investigation on the stability of the hazelnut oil-water emulsion. *J. Dispersion Sci. Technol.* 41 (6), 929–940. <https://doi.org/10.1080/01932691.2019.1614459>.
- Nategh, M., Mahdiyar, H., Malayeri, M.R., Binazadeh, M., 2018. Impact of asphaltene surface energy on stability of asphaltene-toluene system: a parametric study. *Langmuir* 34 (46), 13845–13854. <https://doi.org/10.1021/acs.langmuir.8b02566>.
- Olayiwola, S.O., Dejam, M., 2019. A comprehensive review on interaction of nanoparticles with low salinity water and surfactant for enhanced oil recovery in sandstone and carbonate reservoirs. *Fuel* 241, 1045–1057. <https://doi.org/10.1016/j.fuel.2018.12.122>.
- Oliveira, G.E., Lucas, E.F., 2007. The effect of asphaltenes, naphthenic acids, and polymeric inhibitors on the pour point of paraffins solutions. *J. Dispersion Sci. Technol.* 28 (3), 349–356. <https://doi.org/10.1080/01932690601107526>.
- Redelius, P., 2004. Bitumen solubility model using Hansen solubility parameter. *Energy Fuels* 18, 1087–1092. <https://doi.org/10.1021/ef0400058>.
- Rogel, E., 2016. Asphaltene characterization of paraffinic crude oils. *Fuel* 178, 71–76. <https://doi.org/10.1016/j.fuel.2016.03.030>.
- Shetty, P.P., Daryadel, S., Haire, B.T., Tucker, Z.R., Wu, T., Subramani, V., Morrison, J.J., Quayle, P., Yeates, S., Braun, P.V., Krogstad, J.A., 2019. Low-temperature pack aluminization process on pipeline steel to inhibit asphaltene deposition. *ACS Appl. Mater. Interfaces* 11 (50), 47596–47605. <https://doi.org/10.1021/acsami.9b17430>.
- Shahebrahimi, Y., Fazlali, A., 2018. Experimental and modeling study on precipitated asphaltene biodegradation process using isolated indigenous bacteria. *Ind. Eng. Chem. Res.* 57 (50), 17064–17075. <https://doi.org/10.1021/acs.iecr.8b04661>.
- Tinsley, J.F., 2008. *The Effects of Polymers and Asphaltenes upon Wax Gelation and Deposition*. PhD. Thesis. Princeton University.
- Tinsley, J.F., Prud'homme, R.K., 2010. Deposition apparatus to study the effects of polymers and asphaltenes upon wax deposition. *J. Petrol. Sci. Eng.* 72 (1–2), 166–174. <https://doi.org/10.1016/j.petrol.2010.03.014>.
- Tinsley, J.F., Prud'homme, R.K., Guo, X., Adamson, D.H., Callahan, S., Amin, D., Saini, R., 2007. Novel laboratory cell for fundamental studies of the effect of polymer additives on wax deposition from model crude oils. *Energy Fuels* 21 (3), 1301–1308. <https://doi.org/10.1021/ef060446m>.
- Taheri, S.J., Hosseini, S.A., Kazemzadeh, E., Keshavarz, V., Rajabi, K.M., Naderi, H., 2019. Experimental and mathematical model evaluation of asphaltene fractionation based on adsorption in porous media: dolomite reservoir rock. *Fuel* 245, 570–585. <https://doi.org/10.1016/j.fuel.2019.02.057>.
- Valinejad, R., Nazar, A.R.S., 2013. An experimental design approach for investigating the effects of operating factors on the wax deposition in pipelines. *Fuel* 106, 843–850. <https://doi.org/10.1016/j.fuel.2012.11.080>.
- Venkatesan, R., Ostlund, J., Fogler, H.S., 2003. The effect of asphaltenes on the gelation of waxy Oils. *Energy Fuels* 17, 1630–1640. <https://doi.org/10.1021/ef034013k>.
- Yang, F., Cai, J.Y., Cheng, L., Li, C.X., Ji, Z.Y., Yao, B., Zhao, Y.S., Zhang, G.Z., 2016. Development of asphaltenes-triggered two-layer waxy oil gel deposit under laminar flow: an experimental study. *Energy Fuels* 30, 9922–9932. <https://doi.org/10.1021/acs.energyfuels.6b01482>.
- Yao, Z.W., 2014. *Studies of Asphaltene on Wax-Molecular Mass Transfer Mechanism*. Master. Thesis. China University of Petroleum, Beijing (in Chinese).
- Zhao, B., Shaw, J.M., 2007. Composition and size distribution of coherent nanostructures in Athabasca bitumen and Maya crude oil. *Energy Fuels* 21, 2795–2804. <https://doi.org/10.1021/ef070119u>.